# MyD88 modulates macrophage polarization via p65 NF-κB signaling in early pregnancy loss

YONGHUI JIAO[1], JINGYUAN JIN[2], XIN WU[1], FEN WANG[1], DAN LI[1], NUERADIYE TUSONGJIANG[1] and DIMIN WANG[3]

[1]Department of Reproduction, People's Hospital of Xinjiang Uygur Autonomous Region, Urumqi, Xinjiang Uygur Autonomous Region 830000, P.R. China; [2]Sengong Hospital of Shaanxi Province, Xi'an, Shaanxi 710300, P.R. China; [3]Department of Cardiothoracic Surgery, The First Affiliated Hospital, School of Medicine, Zhejiang University, Hangzhou, Zhejiang 310014, P.R. China

Received May 8, 2026; Accepted November 6, 2026

DOI: 10.3892/br.2026.2228

**Abstract.** Early pregnancy loss (EPL) is a global reproductive health concern. The present study aimed to investigate the role of myeloid differentiation primary response 88 (MyD88) in macrophage polarization during EPL and its implications for pregnancy outcomes. Human decidual tissues were collected from women with normal early pregnancy and patients with EPL. In normal decidual tissue, M2 macrophages predominated, whereas M1 macrophages were significantly increased in EPL tissues. MyD88 expression was significantly higher in EPL decidual tissue at both the mRNA and protein levels. EPL tissues exhibited increased Toll-like receptor (TLR)4 expression, and TLR4 knockdown in THP-1-derived macrophages led to a concurrent decrease in MyD88, suggesting a regulatory link between TLR4 and MyD88. EPL tissues also showed increased levels of M1-associated pro-inflammatory cytokines [including IL-1β, IL-6 and inducible nitric oxide synthase (iNOS)]. MyD88 knockdown in RAW264.7 cells reduced the expression of pro-inflammatory factors (including IL-1β, IL-6 and iNOS) and cluster of differentiation (CD)86 surface marker expression while enhancing the expression of M2 markers (such as CD206 and IL-10). Conversely, MyD88 overexpression in THP-1-derived macrophages significantly increased p65 NF-κB phosphorylation and upregulated pro-inflammatory mediators, which was abrogated by treatment with the NF-κB inhibitor BAY 11-7082. Collectively, the present findings demonstrate that MyD88 upregulation in EPL promotes M1-like macrophage polarization via p65 NF-κB activation, exacerbating decidual inflammation. Targeted downregulation of MyD88 suppressed M1 polarization and enhanced M2 anti-inflammatory responses, suggesting MyD88 as a key regulator of macrophage polarization in the decidua of EPL.

*Correspondence to:* Dr Yonghui Jiao, Department of Reproduction, People's Hospital of Xinjiang Uygur Autonomous Region, 91 Tianchi Road, Urumqi, Xinjiang Uygur Autonomous Region 830000, P.R. China
E-mail: jiaoyonghuixj@126.com

Dr Dimin Wang, Department of Cardiothoracic Surgery, The First Affiliated Hospital, School of Medicine, Zhejiang University, 79 Qingchun Road, Hangzhou, Zhejiang 310014, P. R. China
E-mail: deane14@163.com

*Key words:* early pregnancy loss, macrophage polarization, cluster of differentiation 86, cluster of differentiation 206, myeloid differentiation primary response 88

## Introduction

Early pregnancy loss (EPL), defined as the spontaneous termination of pregnancy before 12 weeks of gestation without medical intervention, remains a significant clinical challenge for reproductive health (1). While chromosomal abnormalities, endocrine dysfunction, environmental factors and immune dysregulation are recognized contributors to EPL pathogenesis (2), emerging evidence highlights the pivotal role of immune mechanisms in maintaining pregnancy (3). Successful gestation requires tightly regulated immune tolerance at the maternal-fetal interface, where an imbalance in decidual immune cell function can disrupt placental development and trigger pregnancy failure (4). Among these cells, decidual macrophages (dMφ) are critical mediators of tissue remodeling and immune homeostasis (5).

dMφ constitute ~20% of the immune cells at the maternal-fetal interface during pregnancy (5). These cells are pivotal for maintaining local immune homeostasis and establishing maternal-fetal tolerance (6), and for facilitating critical processes such as trophoblast invasion, uterine spiral artery remodeling, fetal development and parturition (7). Macrophages exhibit functional plasticity and polarize into two primary subtypes: i) Classically activated M1 (pro-inflammatory); and ii) alternatively activated M2 (anti-inflammatory) macrophages (8). M1 macrophages express surface markers such as cluster of differentiation 86 (CD86) and major histocompatibility complex class II, and secrete pro-inflammatory cytokines such as IL-6 and TNF-α, which mediate tissue inflammation and damage (9). By contrast, M2 macrophages produce immunosuppressive cytokines, including IL-10

and transforming growth factor-β (TGF-β), along with context-dependent levels of IL-6, which collectively sustain immune tolerance and support tissue repair in the gestational microenvironment (10). The dynamic balance between M1 and M2 polarization is tightly regulated by the endometrial microenvironment. Disruption of this equilibrium can trigger pathological inflammation, impair placental development and ultimately contribute to miscarriage (11,12).

Toll-like receptors (TLRs), key sensors of the innate immune system, regulate inflammatory and tolerogenic responses through pathogen- or damage-associated molecular pattern recognition (13). Unlike epithelial cells, macrophages and other immune cells lack epithelial markers; thus, TLR expression in these cells is typically identified via transcriptional profiling (13). By reshaping the tissue microenvironment, TLR signaling modulates inflammatory pathways that are implicated in diverse pathologies, including cancer and autoimmune disorders (14). Myeloid differentiation primary response 88 (MyD88), an adaptor protein, is central to this signaling by mediating downstream TLR-induced activation of NF-κB and subsequent cytokine production (15). MyD88 further governs macrophage polarization, influencing their functional shift between pro-inflammatory (M1) and anti-inflammatory (M2) states in physiological and pathological contexts (16). While the role of MyD88 in TLR-driven inflammation is well-characterized, its contribution to immune tolerance at the maternal-fetal interface, specifically in regulating dMφ polarization during pregnancy, remains poorly understood. The present study aimed to compare dMφ polarization patterns (M1/M2 ratio) in decidual tissues from normal pregnancies and EPL cases, quantify MyD88 expression levels in these cohorts, and elucidate the mechanistic role of MyD88 in modulating dMφ polarization and immune homeostasis during EPL.

## Materials and methods

*Clinical sample*. Decidual tissues were collected from 38 women undergoing elective termination of normal pregnancies (gestational age, 5-11 weeks) and 31 women diagnosed with EPL (gestational age, 7-12 weeks) at the People's Hospital of Xinjiang Uygur Autonomous Region (Urumqi, China) between June 2023 and November 2023. EPL cases were confirmed via comprehensive clinical evaluation, including transvaginal ultrasound and serum β-human chorionic gonadotropin monitoring, alongside symptoms such as vaginal bleeding or cramping. Participants with miscarriages attributable to genetic abnormalities, active infections, thyroid dysfunction, antiphospholipid syndrome or uterine anomalies were excluded. Normal control participants were healthy women with confirmed normal singleton pregnancies who elected to terminate the pregnancy for non-medical reasons. For the normal control group, participants with a history of spontaneous miscarriage, chronic systemic diseases (hypertension, diabetes and autoimmune disorders), thyroid dysfunction, active infections, TORCH infections, hormonal or immunosuppressive therapy within 3 months, and any pregnancy complications were excluded. The EPL group included patients with and without a history of miscarriage, as detailed in Table SI. All control participants were generally healthy at the time of tissue collection. The clinicopathological data has been provided in Table SI. The study protocol was approved by the Ethics Committee of the People's Hospital of Xinjiang Uygur Autonomous Region (approval no. KY2023060138), and all participants provided written informed consent prior to tissue collection.

*Cell culture*. The murine macrophage RAW264.7 cell line (American Type Culture Collection) was cultured in Dulbecco's modified Eagle's medium (cat. no. 11965092; Gibco; Thermo Fisher Scientific, Inc.) supplemented with 10% fetal bovine serum (FBS; cat. no. 10099141; Gibco; Thermo Fisher Scientific, Inc.) and 1% penicillin/streptomycin (cat. no. 60162ES; Shanghai Yeasen Biotechnology Co., Ltd.). Cells were maintained at 37˚C in a humidified atmosphere containing 5% $CO_2$. All experiments utilized cells at passages 3-10 to ensure phenotypic stability. Human monocytic THP-1 cells were cultured in RPMI-1640 medium supplemented with 10% FBS and 1% penicillin/streptomycin at 37˚C in a humidified atmosphere containing 5% $CO_2$. For differentiation into macrophages, THP-1 cells were treated with 100 ng/ml phorbol 12-myristate 13-acetate for 48 h at 37˚C. After differentiation, adherent macrophages were washed and rested in fresh medium for 24 h prior to subsequent experiments.

*Plasmid, transfection and treatment*. Small interfering RNA targeting MyD88 (si-MyD88) and TLR4 (si-TLR4), and a scrambled negative control siRNA (si-NC) were synthesized by Sangon Biotech Co., Ltd, with the following sequences: si-MyD88 sense, AAGCGACUGAUUCCUAUUAAAtt and antisense, UUUAAUAGGAAUCAGUCGCUUtt; si-TLR4 sense, GUGGCUCACAAUCUUAUCCAAtt and antisense, UUGGAUAAGAUUGUGAGCCACtt; si-IL-1R sense, CCG GUUGUUAAAACUGGUUUAtt and antisense, UAAACC AGUUUUAACAACCGGtt; and si-NC sense, UUACCA ACGUGUCAAUGCGUAtt and antisense, UACGCAUUG ACACGUUGGUAAtt. Lyophilized siRNA was reconstituted in 400 $\mu$l RNase-free water to achieve a stock concentration of 20 $\mu$M. The human and mouse MyD88 coding sequences were cloned into the pcDNA3.1 expression vector (Youbio Co., Ltd.). THP-1-derived macrophages and RAW264.7 cells were separately transfected with either 2 $\mu$g of the MyD88 overexpression plasmid or 2 $\mu$g of the empty pcDNA3.1 vector as a negative control. RAW264.7 cells were transfected with si-MyD88 or si-NC (as a negative control) at a concentration of 50 nM. Transfection was performed using Lipofectamine 3000 (Invitrogen; Thermo Fisher Scientific, Inc.) according to the manufacturer's instructions. Cells were incubated at 37˚C for 6 h during transfection, and subsequent experiments were performed at 48 h post-transfection. To investigate whether the pro-inflammatory effects of MyD88 were mediated through the NF-κB pathway, MyD88-overexpressing THP-1-derived macrophages were treated with the specific NF-κB inhibitor BAY 11-7082 (cat. no. HY-13453; MedChemExpress). Cells were incubated with 10 $\mu$M BAY 11-7082 or DMSO as a vehicle control for 1 h at 37˚C prior to treatment with MyD88-overexpressing vector.

*Western blot*. Total proteins were extracted from decidual tissues (normal and EPL) and transfected cells (RAW264.7 cells and THP-1-derived macrophages). The cells and tissues

were lysed on ice for 20 min using 100 $\mu$l RIPA buffer (cat. no. P0013B; Beyotime, Inc.) supplemented with 1 mM phenylmethylsulfonyl fluoride (cat. no. ST506; Beyotime, Inc.). Lysates were centrifuged at 12,000 x g for 15 min at 4˚C, and supernatants were collected. Protein concentrations were quantified via BCA assay (cat. no. 23225; Thermo Fisher Scientific, Inc.). Equal amounts of protein (20-30 $\mu$g) were resolved on 10% gels using SDS-PAGE and transferred to polyvinylidene difluoride membranes (cat. no. IPVH00010; Merck KGaA). The membranes were blocked with 5% non-fat milk in Tris-buffered saline containing 0.1% TBST for 1 h at room temperature, then incubated overnight at 4˚C with the following primary antibodies: Anti-MyD88 (1:1,000; cat. no. ab131071; Abcam; Danaher), anti-TLR4 (1:1,000; cat. no. sc-293072; Santa Cruz Biotechnology), anti-IL-1R (1:1,000; cat. no. sc-393998; Santa Cruz Biotechnology, Inc.), anti-phospho-p65 (Ser536; 1:1,000; cat. no. 93H1; Cell Signaling Technology, Inc.), anti-p65 (1:1,000; cat. no. D14E12; Cell Signaling Technology, Inc.) and anti-β-actin (1:5,000; cat. no. 66009-1-Ig; Proteintech, Inc.). After three washes with TBST, the membranes were incubated with horseradish peroxidase (HRP)-conjugated secondary antibodies (1:7,500; cat. no. SA00001-2; Proteintech Group, Inc.) for 1 h at room temperature. Protein bands were visualized using an enhanced chemiluminescence detection system (cat. no. AB180-5001; Tanon Science and Technology Co., Ltd.), and densitometric analysis was performed with ImageJ software (version 1.4; National Institutes of Health).

*Reverse transcription-quantitative (RT-q)PCR*. Total RNA was extracted from decidual tissues (normal and EPL) and transfected cells (RAW264.7 cells and THP-1-derived macrophages) using TRIzol® reagent (cat. no. 15596026; Invitrogen; Thermo Fisher Scientific, Inc.) and reverse-transcribed into cDNA with a PrimeScript™ RT Reagent Kit (cat. no. RR037A; Takara Bio, Inc.) according to the manufacturer's instructions (37˚C for 15 min, followed by 85˚C for 5 sec). Quantitative PCR was performed in triplicate using a QuantiNova SYBR Green PCR Kit (cat. no. 208054; Qiagen, Inc.) on a Bio-Rad CFX96 Real-Time PCR System (Bio-Rad Laboratories, Inc.). Each 20-$\mu$l reaction contained 10 $\mu$l SYBR Green mix, 2 $\mu$l cDNA template, 0.8 $\mu$l forward/reverse primers and 7.2 $\mu$l nuclease-free water. Cycling conditions were as follows: Initial denaturation at 95˚C for 5 min; 40 cycles of 95˚C for 30 sec, 60˚C for 40 sec and 72˚C for 1 min; and a final extension at 72˚C for 10 min. Relative gene expression was calculated using the $2^{-\Delta\Delta Cq}$ method (17), with β-actin as the endogenous control. Primer sequences are provided in Table SII. To ensure species-specific amplification, human-specific primers were used for experiments involving human decidual tissues and THP-1-derived macrophages, while mouse-specific primers were used for experiments involving RAW264.7 cells.

*Flow cytometry*. Decidual tissues were enzymatically dissociated using collagenase IV (1 mg/ml; cat. no. 17104019; Gibco; Thermo Fisher Scientific, Inc.) and DNase I (100 U/ml; cat. no. DN25; Sigma-Aldrich; Merck KGaA) in RPMI-1640 medium for 45 min at 37˚C (18,19). Single-cell suspensions were filtered through a 70-$\mu$m strainer and enriched for leukocytes via Ficoll-Paque™ PLUS density gradient centrifugation (cat. no. 17144003; Cytiva). Cells were cultured overnight in RPMI-1640 medium. For surface marker staining, cells were blocked with Human TruStain FcX™ (cat. no. 422302; BioLegend, Inc.) for 10 min at 4˚C and stained with the following fluorochrome-conjugated antibodies for 30 min at 4C in the dark: Anti-CD45 APC-Cy7 (clone HI30; cat. no. 304014; 1:100; BioLegend, Inc.), anti-CD14 FITC (clone M5E2; cat. no. 301804; 1:200; BioLegend, Inc.), anti-CD86 PE (clone IT2.2; cat. no. 305406; 1:100; BioLegend, Inc.), anti-CD206 PerCP-Cy5.5 (clone 15-2; cat. no. 321120; 1:50; BioLegend, Inc.), anti-CD163 BV421 (clone GHI/61; cat. no. 333612; 1:100; BioLegend, Inc.) and anti-CD209 APC (clone 9E9A8; cat. no. 330108; 1:100; BioLegend, Inc.). Live/dead discrimination was performed using the Zombie NIR™ Fixable Viability Kit (cat. no. 423106; BioLegend, Inc.). To address the heterogeneity of dMφ, $CD86^+CD206^-$ cells were identified as M1-like, $CD86^-CD206^+$ cells as M2-like and $CD86^+CD206^+$ cells as a mixed-phenotype population. For refined classification, M1-like macrophages were identified as $CD45^+CD14^+CD86^+CD206^-CD163^-CD209^-$cells, and M2-like macrophages were identified as $CD45^+CD14^+CD86^-CD206^+CD163^+CD209^+$ cells. Cells were analyzed on a BD FACS Aria™ II flow cytometer (BD Biosciences) with FlowJo software (version 10; FlowJo LLC).

*ELISA*. Pro- and anti-inflammatory cytokine levels in decidual tissue homogenates and cell culture supernatants were quantified using ELISA. Tissues were homogenized in ice-cold PBS containing 1X protease inhibitor cocktail (cat. no. 11873580001; Roche Diagnostics) and centrifuged at 10,000 x g for 15 min at 4˚C. Supernatants were collected and stored at -80˚C until analysis. The following cytokines were measured using commercial ELISA kits according to the manufacturer's protocols: IL-1β (cat. no. DLB50/MLB00C; R&D Systems; Bio-Techne), IL-6 (cat. no. D6050/M6000B; R&D Systems; Bio-Techne), iNOS (cat. no. NBP2-80255/NBP2-80256; R&D Systems; Bio-Techne), IL-4 (cat. no. D4050/M4000B; R&D Systems; Bio-Techne) and IL-10 (cat. no. D1000B/M1000B; R&D Systems; Bio-Techne). Cytokine concentrations were normalized to total protein content. Absorbance was measured at 450 nm using a SpectraMax® M5 microplate reader (Molecular Devices LLC). Standard curves were generated for each plate, and data were analyzed using SoftMax® Pro software (version 7.1; Molecular Devices LLC). All assays were performed in triplicate.

*Immunohistochemistry*. Decidual tissues were fixed in 4% paraformaldehyde (PFA; cat. no. 158127; Sigma-Aldrich; Merck KGaA) for 24 h at room temperature, paraffin-embedded and sectioned into 5-$\mu$m slices using a microtome. Antigen retrieval was performed by incubating deparaffinized sections in citrate-based buffer (pH 6.0) at 100˚C for 20 min. Sections were blocked with 5% bovine serum albumin (BSA; cat. no. A7906; Sigma-Aldrich; Merck KGaA) for 1 h at room temperature, and then incubated overnight at 4˚C with the following primary antibodies: Anti-IL-1β (cat. no. P420B; 1:200; Invitrogen; Thermo Fisher Scientific, Inc.), anti-iNOS (1:200; cat. no. ab283655; Abcam; Danaher), anti-IL-10 (1:200; cat. no. 14-7108-81; Invitrogen; Thermo Fisher Scientific, Inc.) and anti-MyD88 (1:200; cat. no. ab131071;

Abcam; Danaher). Immunoreactivity was visualized using species-matched HRP-conjugated secondary antibodies (1:500; cat. no. MP-7401-15 for rabbit or MP-7404-50 for rat; Vector Laboratories, Inc.) incubated at room temperature for 1 h, followed by visualization with a DAB Substrate Kit (cat. no. SK-4100; Vector Laboratories, Inc.). Images were captured using a light microscope (Olympus Corporation).

*Immunofluorescence*. RAW264.7 cells grown on glass coverslips were fixed with 4% PFA (cat. no. 158127; Sigma-Aldrich; Merck KGaA) for 30 min at room temperature. After three washes with PBS, cells were permeabilized with 0.3% Triton X-100 (cat. no. T8787; Sigma-Aldrich; Merck KGaA) in PBS for 1 h at room temperature. Non-specific binding was blocked with 5% BSA (cat. no. A7906; Sigma-Aldrich; Merck KGaA) in PBS for 1 h at room temperature. Cells were incubated overnight at 4˚C with the following primary antibodies diluted in blocking buffer: Anti-IL-1β (1:200; cat. no. P420B; Invitrogen; Thermo Fisher Scientific, Inc.), anti-CD86 (M1 marker; cat. no. 305406; clone IT2.2; 1:200; BioLegend, Inc.) and anti-CD206 (M2 marker; 1:200; cat. no. 321102; clone 15-2; BioLegend, Inc.). To assess p65 NF-κB nuclear translocation, THP-1-derived macrophages grown on glass coverslips were fixed with 4% PFA for 15 min, permeabilized with 0.3% Triton X-100 for 10 min and blocked with 5% BSA for 1 h at room temperature. After which, the cells were incubated overnight at 4˚C with an anti-p65 NF-κB primary antibody (1:200; Cell Signaling Technology, Inc.). After PBS washes, cells were incubated with Alexa Fluor® 488-conjugated secondary antibodies (1:500; cat. no. A-11008; Invitrogen; Thermo Fisher Scientific, Inc.) for 1 h at room temperature in the dark. Nuclei were counterstained with 4',6-diamidino-2-phenylindole (1 $\mu$g/ml; cat. no. D9542; Sigma-Aldrich; Merck KGaA) at room temperature for 10 min. Coverslips were mounted with ProLong™ Gold Antifade Mountant (cat. no. P36930; Invitrogen; Thermo Fisher Scientific, Inc.). Images were captured using an Olympus FV3000 confocal microscope (Olympus Corporation). Fluorescence intensity was quantified using ImageJ software (version 1.4; National Institutes of Health).

*Statistical analysis*. Statistical analyses were performed using GraphPad Prism software (version 8.0; Dotmatics). Data are presented as the mean ± standard deviation. Normality was assessed using the Shapiro-Wilk test. For comparisons between two independent groups, an unpaired two-tailed Student's t-test was applied when the data met the assumptions of normality and equal variance. When the normality assumption was violated, the non-parametric Mann-Whitney U test was applied. Effect sizes ($\varepsilon^2$ and $R^2$) and 95% confidence intervals (CIs) are reported in the figure legend. For comparisons among multiple groups, one-way analysis of variance followed by Tukey's post hoc test was used. P<0.05 was considered to indicate a statistically significant difference.

## Results

*M1-like macrophage proportion is elevated in the decidual tissue of EPL cases*. To investigate macrophage polarization dynamics in EPL, the M1-like and M2-like macrophage subsets in decidual tissues from EPL and normal pregnancy cohorts were analyzed via flow cytometry. Gating strategies for identifying M1-like macrophages (pro-inflammatory) and M2-like macrophages (anti-inflammatory) macrophages, along with representative flow plots, are illustrated in Fig. 1A-E. Compared with that in normal pregnancies, the proportion of $CD45^+CD14^+CD86^-CD206^+$ M2-like macrophages was markedly lower in EPL tissues (Fig. 1F; P<0.0001). Conversely, the frequency of $CD45^+CD14^+CD86^+CD206^-$ M1-like macrophages was substantially increased in EPL decidua (Fig. 1G; P<0.0001). Notably, the proportion of the $CD45^+CD14^+CD86^+CD206^+$ mixed-phenotype population showed no significant difference between the two groups (Fig. 1H; P=0.0621). To further characterize these subsets with higher specificity and address the heterogeneity of dMφ, a four-marker gating strategy was employed. Within the $CD45^+CD14^+$ population, M2-like macrophages were further defined as $CD86^-CD206^+CD163^+CD209^+$, and M1-like macrophages were defined as $CD86^+CD206^-CD163^-CD209^-$. Consistently, the proportion of the $CD86^-CD206^+CD163^+CD209^+$ M2-like subset was significantly decreased (Fig. 1I; P<0.0001), whereas the proportion of the $CD86^+CD206^-CD163^-CD209^-$ M1-like subset was significantly elevated in the EPL decidua compared with that in normal pregnancies (Fig. 1J; P<0.0001). Collectively, these data demonstrate a robust shift toward a pro-inflammatory M1-like-dominant phenotype in EPL decidua, indicating that aberrant macrophage polarization is involved in the pathogenesis of EPL.

*Pro-inflammatory M1 polarization dominance characterizes the decidual microenvironment in EPL*. To assess the functional impact of macrophage polarization in EPL, pro-inflammatory (M1) and anti-inflammatory (M2) factors were quantified in decidual tissues. Immunohistochemical analysis revealed a distinct inflammatory imbalance in EPL decidua. Compared with normal controls, EPL tissues exhibited a significant increase in the number of IL-1β-positive cells (Fig. 2A and B; P<0.0001), which was parallel to the increase in $iNOS^+$ cell infiltration (Fig. 2D and E; P<0.01). By contrast, the proportion of immunoregulatory IL-10-positive cells was markedly reduced in patients with EPL (Fig. 2G and H; P<0.001), underscoring a pathological shift toward pro-inflammatory dominance at the maternal-fetal interface. Consistent with these findings, the results of the ELISA revealed a pronounced inflammatory milieu in EPL, with significantly elevated levels of M1-associated mediators, including IL-1β (Fig. 2C; P<0.001), iNOS (Fig. 2F; P<0.01) and IL-6 (Fig. 2J; P<0.01) compared with those in normal controls. Conversely, the anti-inflammatory cytokines IL-10 and IL-4, which are hallmarks of M2 macrophages, exhibited markedly reduced levels in EPL tissues compared with those in normal controls (Fig. 2I; P<0.01 and K; P<0.01). Collectively, these results highlight a pathological shift toward M1-driven inflammation in EPL, characterized by elevated levels of pro-inflammatory mediators and diminished M2-associated immunosuppression.

*MyD88 is upregulated in EPL decidual tissue*. MyD88, a central adaptor protein in TLR/IL-1R signaling, serves as a critical regulator of inflammatory responses and macrophage polarization dynamics. To investigate its involvement in dMφ

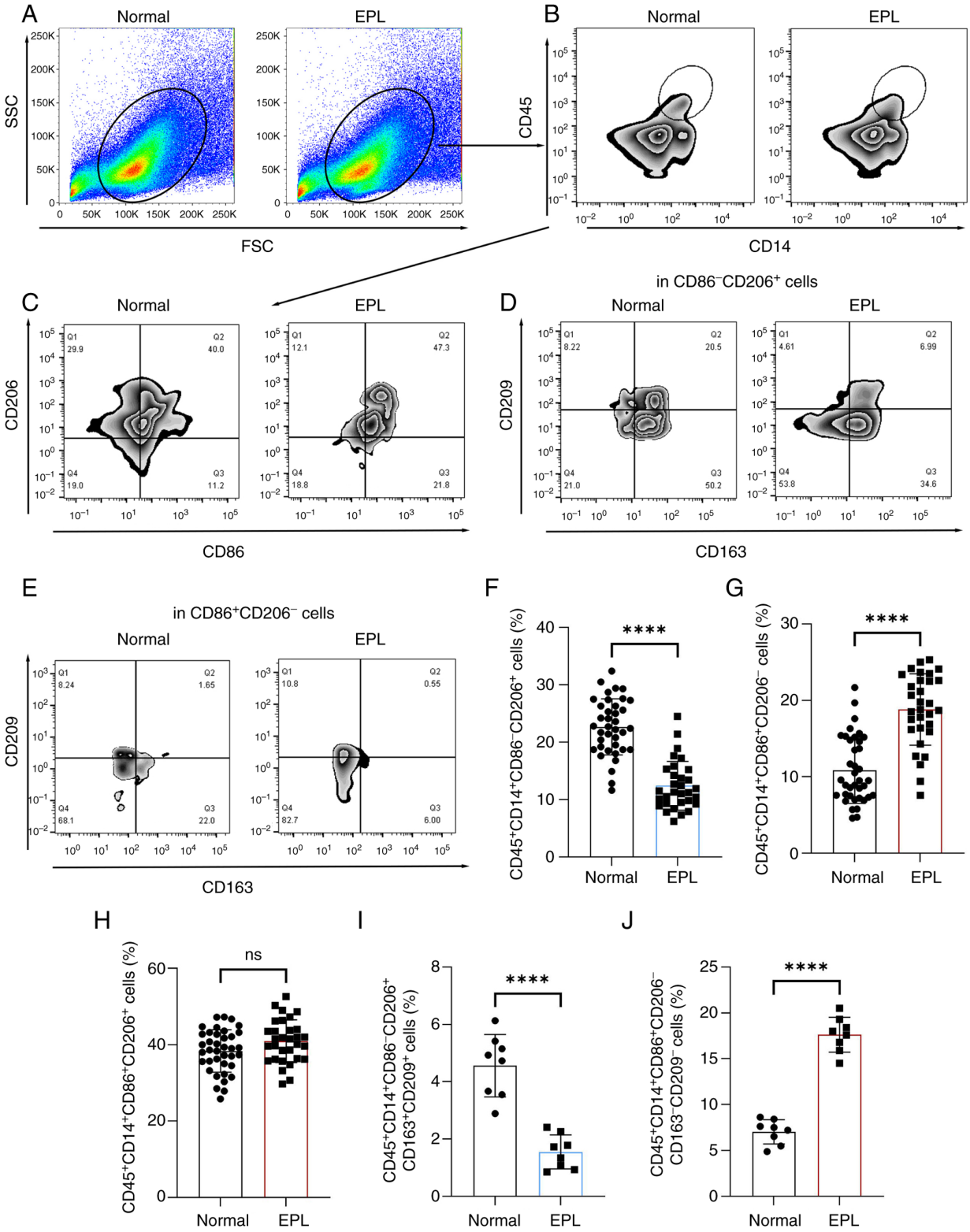



Figure 1. M1-like macrophage proportion is elevated in decidual tissue of EPL. (A) Representative flow cytometry plots illustrating the gating strategy based on forward scatter (FSC) and side scatter (SSC). (B) Gating strategy for $CD14^+CD45^+$ cells. (C) Representative flow cytometry plots showing $CD86^+CD206^-$ and $CD86^-CD206^+$ cell populations. (D) Representative flow cytometry plots illustrating $CD163^+CD209^+$ cells within the $CD86^-CD206^+$ population. (E) Representative flow cytometry plots illustrating $CD163^+CD209^+$ cells within the $CD86^+CD206^-$ population. (F) The proportion of $CD45^+CD14^+CD86^-CD206^+$ cells was determined in decidual tissue of normal patients (n=38 normal deciduas) and those with EPL (n=31 EPL deciduas) ($^{****}$P<0.0001, unpaired t-test; 95% CI, -12.50 to -8.040; $R^2$=0.5577). (G) The proportion of $CD45^+CD14^+CD86^+CD206^-$ cells was evaluated in decidual tissue of normal patients (n=38 normal deciduas) and thoe with EPL (n=31 EPL deciduas) ($^{****}$P<0.0001, Mann-Whitney U test; Hodges-Lehmann estimate of difference, 8.600; 95% CI, 6.100 to 10.70). (H) The proportion of $CD45^+CD14^+CD86^+CD206^+$ cells was determined in decidual tissue of normal patients (n=38 normal deciduas) and those with EPL (n=31 EPL deciduas) (P=0.0621, unpaired t-test; 95% CI, -0.1333 to 5.250; $R^2$=0.051). (I) The proportion of $CD45^+CD14^+CD86^-CD206^+CD163^+CD209^+$ M2-like macrophages was evaluated in decidual tissue of normal patients and those with EPL (n=8 deciduas) ($^{****}$P<0.0001, unpaired t-test; 95% CI, -3.953 to -2.070; $R^2$=0.7708). (J) The proportion of $CD45^+CD14^+CD86^+CD206^-CD163^-CD209^-$ M1-like macrophages was evaluated in decidual tissue of normal patients and those with EPL (n=8 deciduas) ($^{****}$P<0.0001, unpaired t-test; 95% CI, 8.831 to 12.34; $R^2$=0.9227). EPL, early pregnancy loss; FSC, forward scatter; SSC, side scatter; CD, cluster of differentiation; ns, not significant.

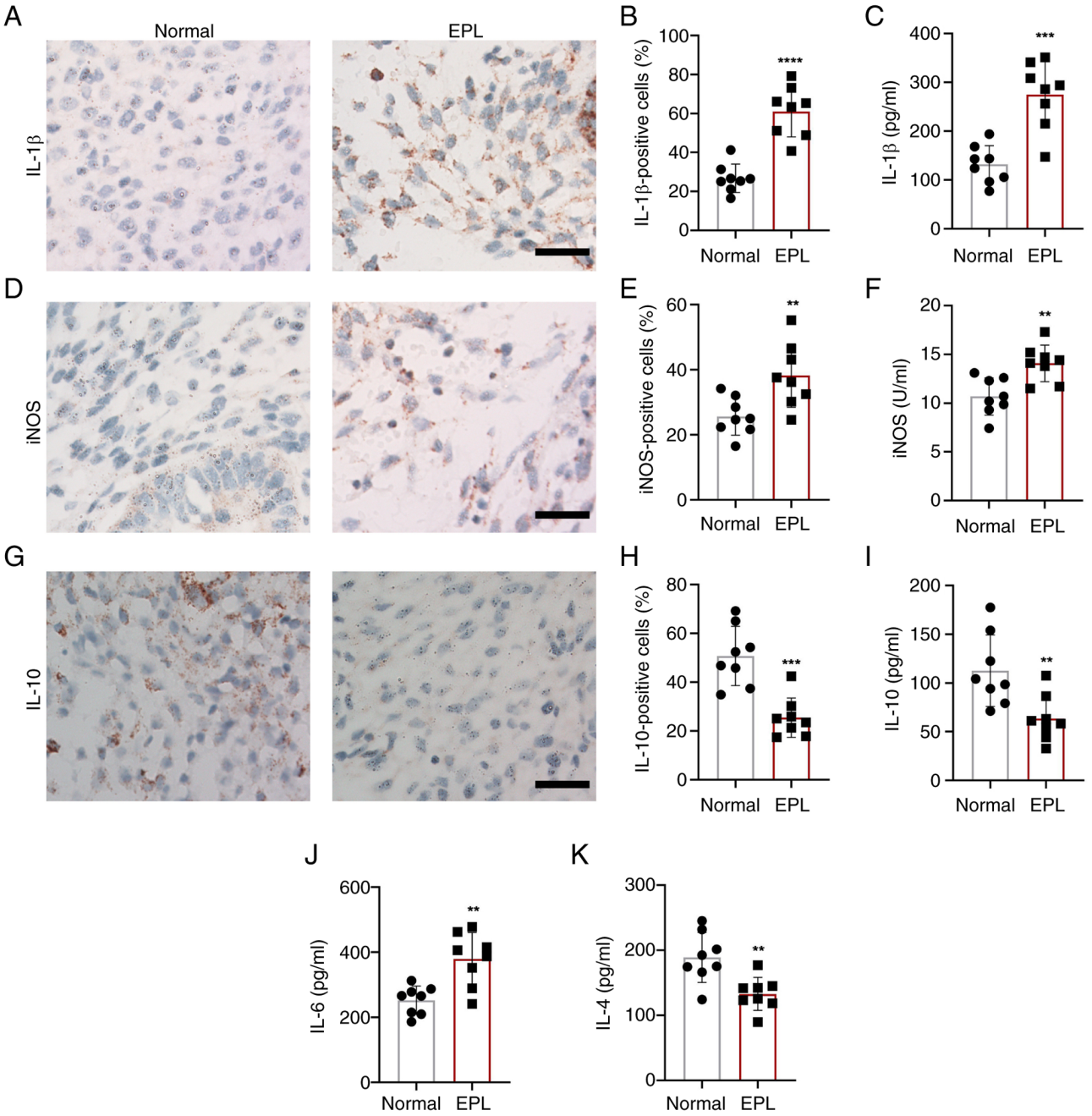



Figure 2. Pro-inflammatory M1 polarization dominance characterizes the decidual microenvironment in EPL. (A and B) Immunohistochemical analysis and quantification of IL-1β in normal controls and patients with EPL (n=8 deciduas) (scale bar, 50 $\mu$m; $^{****}$P<0.0001, unpaired t-test; 95% CI, 22.96 to 45.57; $R^2$=0.7512). (C) The inflammatory cytokines IL-1β were detected in normal controls and patients with EPL (n=8 deciduas) ($^{***}$P<0.001, unpaired t-test; 95% CI, 84.38 to 202.5; $R^2$=0.6595). (D and E) Immunohistochemical analysis and quantification of iNOS in normal controls and patients with EPL (n=8 deciduas) (scale bar, 50 $\mu$m; $^{**}$P<0.01, unpaired t-test; 95% CI, 3.990 to 21.24; $R^2$=0.4128). (F) The inflammatory mediators iNOS were detected in normal controls and patients with EPL (n=8 deciduas) ($^{**}$P<0.01, unpaired t-test; 95% CI, 1.372 to 5.428; $R^2$=0.4801). (G and H) Immunohistochemical analysis and quantification of IL-10 in normal controls and patients with EPL (n=8 deciduas) (scale bar, 50 $\mu$m; $^{***}$P<0.001, unpaired t-test; 95% CI, -36.33 to -14.24; $R^2$=0.6326). (I) The anti-inflammatory factors IL-10 were detected in normal controls and patients with EPL (n=8 deciduas) ($^{**}$P<0.01, unpaired t-test; 95% CI, -82.32 to -16.05; $R^2$=0.4200). (J) The inflammatory cytokines IL-6 were detected in normal controls and patients with EPL (n=8 deciduas) ($^{**}$P<0.01, unpaired t-test; 95% CI, 56.16 to 196.8; $R^2$=0.5153). (K) The anti-inflammatory factors IL-4 were detected in normal controls and patients with EPL (n=8 deciduas) ($^{**}$P<0.01, unpaired t-test; 95% CI, -90.90 to -21.15; $R^2$=0.4589). EPL, early pregnancy loss; iNOS, inducible nitric oxide synthase.

dysregulation during EPL, MyD88 expression was systematically analyzed in decidual tissues. Immunohistochemical quantification revealed a striking 2.1-fold increase in the number of MyD88-positive cells in EPL decidua compared with that in normal controls (Fig. 3A and B; P<0.0001). Consistently, immunoblotting confirmed a 1.4-fold increase in MyD88 protein abundance in EPL decidua compared with that in normal controls (Fig. 3C and E; P<0.001). The protein expression of TLR4 was also significantly increased in EPL decidual tissues (Fig. 3C and D; P<0.01). RT-qPCR demonstrated a 2.2-fold upregulation of *MyD88* mRNA expression in EPL decidua compared with that in normal controls (Fig. 3F; P<0.001). To preliminarily explore the relationship between TLR4 and MyD88 expression, an *in vitro* validation was

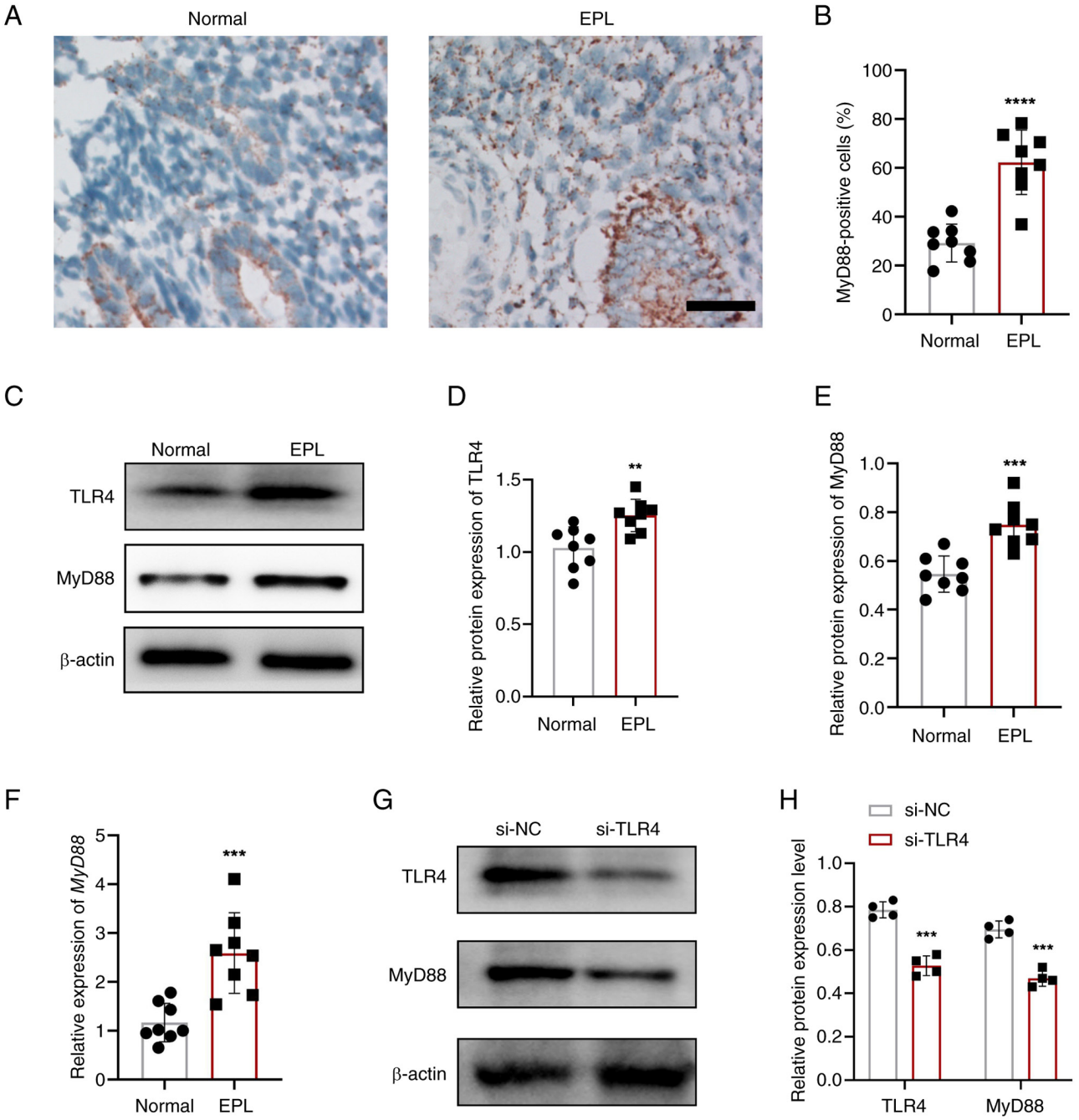



Figure 3. MyD88 was upregulated in EPL decidual tissue. (A and B) Immunohistochemical analysis and quantification of MyD88 in (A) normal controls and (B) patients with EPL (n=8 deciduas) (scale bar, 50 $\mu$m; $^{****}$P<0.0001, unpaired t-test; 95% CI, 21.47 to 44.68; $R^2$=0.7273). The (C) protein expression and (D) quantification of TLR4 ($^{**}$P<0.01, unpaired t-test; 95% CI, 0.08538 to 0.3646; $R^2$=0.4604) and (E) MyD88 were determined in decidual tissue of patients with EPL (n=8 deciduas) ($^{***}$P<0.001, unpaired t-test; 95% CI, 0.1137 to 0.2913; $R^2$=0.6306). (F) The mRNA expression levels of *MyD88* were determined in decidual tissue of patients with EPL (n=8 deciduas) ($^{***}$P<0.001, unpaired t-test; 95% CI, 0.7310 to 2.119; $R^2$=0.5808). The (G) protein expression and (H) quantification of TLR4 ($^{***}$P<0.001, unpaired t-test; 95% CI, -0.3294 to -0.1856; $R^2$=0.9274) and MyD88 ($^{***}$P<0.001, unpaired t-test; 95% CI, -0.2909 to -0.1591; $R^2$=0.9209) were determined in si-TLR4-treated THP-1-derived macrophages (n=4 independent experiments). Myd88, myeloid differentiation primary response 88; EPL, early pregnancy loss; si-, small interfering RNA; NC, negative control; TLR4, Toll-like receptor 4.

performed in THP-1-derived macrophages. Knockdown of TLR4 using a specific siRNA (si-TLR4) led to a concurrent decrease in the protein expression of both TLR4 and MyD88 (Fig. 3G and H; P<0.001), suggesting that the increase in MyD88 expression observed in EPL tissues may be associated with upstream TLR4 signaling. By contrast, knockdown of IL-1R using si-IL-1R significantly reduced IL-1R protein levels but did not alter MyD88 expression (Fig. S1A and B; P<0.001 for IL-1R; P=0.1999 for MyD88). These results indicate that TLR4, but not IL-1R, is involved in regulating MyD88 expression in macrophages.

*MyD88 knockdown attenuates pro-inflammatory macrophage activation in RAW264.7 cells*. To investigate the functional role of MyD88 in macrophage polarization, MyD88 expression was silenced in murine RAW264.7

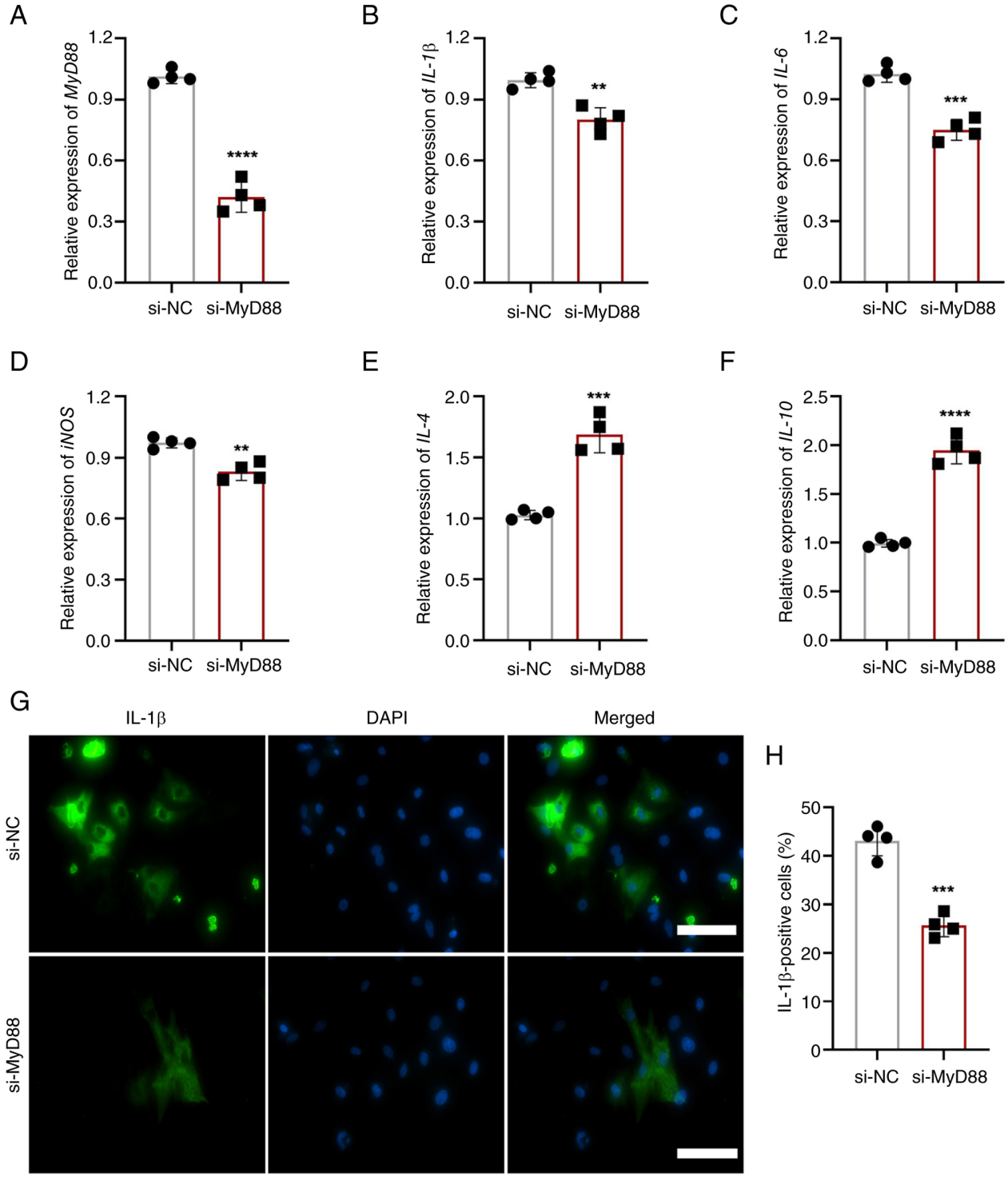



Figure 4. MyD88 knockdown attenuates pro-inflammatory macrophage activation in RAW264.7 cells. (A) The mRNA levels of *MyD88* were determined following si-MyD88 or si-NC treatment in RAW264.7 cells (n=4 independent experiments) (****P<0.0001, unpaired t-test; 95% CI, -0.6926 to -0.4924; $R^2$=0.9722). The mRNA levels of inflammatory mediators (B) *IL-1β* (**P<0.01, unpaired t-test; 95% CI, -0.2806 to -0.1094; $R^2$=0.8380), (C) *IL-6* (***P<0.001, unpaired t-test; 95% CI, -0.3552 to -0.1948; $R^2$=0.9214) and (D) *iNOS* (**P<0.01, unpaired t-test; 95% CI, -0.2027 to -0.08225; $R^2$=0.8481) were detected following si-MyD88 or si-NC treatment in RAW264.7 cells (n=4 independent experiments). The mRNA expression levels of anti-inflammatory cytokine (E) *IL-4* (***P<0.001, unpaired t-test; 95% CI, 0.4708 to 0.8492; $R^2$=0.9239) and (F) *IL-10* (****P<0.0001, unpaired t-test; 95% CI, 0.7775 to 1.127; $R^2$=0.9673) were detected following si-MyD88 or si-NC treatment in RAW264.7 cells (n=4 independent experiments). (G) Immunofluorescence staining and (H) quantification of IL-1β following si-MyD88 or si-NC treatment in RAW264.7 cells (n=4 independent experiments) (scale bar, 50 $\mu$m; ***P<0.001, unpaired t-test; 95% CI, -22.27 to -12.75; $R^2$=0.9310). MyD88, myeloid differentiation primary response 88; si-, small interfering RNA; NC, negative control; iNOS, inducible nitric oxide synthase.

macrophages using siRNA. Compared with scrambled siRNA (si-NC), successful knockdown resulted in a 60% reduction in *MyD88* mRNA levels (Fig. 4A; P<0.0001). MyD88 suppression significantly altered the expression profiles of inflammatory mediators, whereby the expression levels of the proinflammatory mediators *IL-1β* (Fig. 4B; P<0.01), *IL-6*

(Fig. 4C; P<0.001), and *iNOS* (Fig. 4D; P<0.01) were significantly reduced in MyD88-knockdown cells. The expression levels of anti-inflammatory mediators *IL-4* (Fig. 4E; P<0.001) and *IL-10* (Fig. 4F; P<0.0001) were significantly increased compared with those in the controls. The suppressive effect of MyD88 knockdown on IL-1β levels was further confirmed at the cellular level by immunofluorescence staining. The number of IL-1β-positive cells was significantly decreased in si-MyD88-transfected cells compared with that in si-NC control cells (Fig. 4G and H; P<0.001). The suppression of IL-1β, IL-6 and iNOS, hallmarks of M1 polarization, alongside the induction of IL-4 and IL-10, which are key M2-associated cytokines, suggests that MyD88 is a critical regulator of macrophage functional plasticity.

*MyD88 overexpression promotes pro-inflammatory macrophage activation in THP-1-derived macrophages via p65 NF-κB*. To further validate the functional role of MyD88 in macrophage polarization, MyD88 overexpression experiments were performed in RAW264.7 cells. Successful overexpression of MyD88 was confirmed by western blot analysis, showing significantly increased MyD88 protein levels in MyD88-overexpressing cells compared with those in the controls (Fig. S1C and D; P<0.0001). Moreover, it was found that MyD88 overexpression led to a marked upregulation of pro-inflammatory mediators. The proportions of IL-1β (Fig. S1E; P<0.01), iNOS (Fig. S1F; P<0.01) and IL-6 (Fig. S1G; P<0.01) cytokines were significantly increased in MyD88-overexpressing cells compared with those in the controls. By contrast, the proportions of the anti-inflammatory cytokines IL-4 and IL-10 were significantly decreased by MyD88 overexpression (Fig. S1H; P<0.01 and I; P<0.01). The NF-κB pathway mediates the regulation of macrophage polarization by MyD88 (20,21). To directly investigate whether MyD88 regulates macrophage polarization through the NF-κB pathway, a gain-of-function analysis was performed in THP-1-derived macrophages. Notably, immunofluorescence staining confirmed that MyD88 overexpression promoted the nuclear translocation of p65 NF-κB, as evidenced by the increased co-localization of p65 with the nuclei (Fig. 5A). Overexpression of MyD88 successfully upregulated its protein level and led to a significant increase in the ratio of p65 NF-κB (p-p65)/total p65 compared with control cells (Fig. 5B and C; P<0.001 for MyD88; P<0.001 for p-p65/total p65). To determine whether the observed pro-inflammatory phenotype was specifically dependent on NF-κB activation, MyD88-overexpressing cells were treated with the specific NF-κB inhibitor BAY 11-7082. The inhibitor effectively suppressed the MyD88-driven elevation of p-p65 (Fig. 5D and E; P<0.001 for p-p65/total p65), confirming that MyD88 acts upstream of NF-κB phosphorylation. The upregulation of key pro-inflammatory mediators IL-1β (Fig. 5F; P<0.01), IL-6 (Fig. 5G; P<0.05) and iNOS (Fig. 5H; P<0.05) induced by MyD88 overexpression was markedly attenuated upon BAY 11-7082 treatment. By contrast, the expression levels of the anti-inflammatory cytokines IL-4 (Fig. 5I; P<0.01) and IL-10 (Fig. 5J; P<0.05) were significantly increased by NF-κB inhibition. Collectively, these results demonstrate that MyD88 overexpression drives a pro-inflammatory response in macrophages, which is specifically mediated through the activation of the p65 NF-κB pathway.

*MyD88 knockdown suppresses M1 polarization while concurrently promoting M2 polarization in RAW264.7 cells*. To further elucidate the role of MyD88 in M1 polarization, MyD88 was silenced and CD86 expression was evaluated in RAW264.7 cells. Immunofluorescence staining showed a significant reduction in CD86 fluorescence intensity in MyD88-knockdown cells compared with that in si-NC controls. Quantitative analysis demonstrated an 85% decrease in CD86 expression (Fig. 6A and B; P<0.001). These results confirm that MyD88 downregulation suppresses M1 polarization, as evidenced by diminished CD86 expression. To investigate the role of MyD88 in M2 polarization, MyD88 was silenced and CD206 expression was evaluated in RAW264.7 cells. Immunofluorescence staining showed a significant increase in CD206 fluorescence intensity in MyD88-knockdown cells compared with that in si-NC controls. Quantitative analysis revealed a six-fold upregulation of CD206 expression (Fig. 6C and D; P<0.0001). These findings indicate that MyD88 suppression shifts macrophage polarization toward an anti-inflammatory M2 phenotype. Enhanced CD206 expression, coupled with the observations of reduced M1 markers (such as CD86, IL-1β and IL-6) and elevated M2-associated cytokines (such as IL-4 and IL-10), highlights MyD88 as a pivotal regulator of macrophage plasticity. This dual modulation suggests that targeting MyD88 could rebalance decidual immune homeostasis, potentially mitigating inflammation-driven pregnancy loss.

## Discussion

Macrophages at the maternal-fetal interface exhibit distinct functional polarization, whereby M1 macrophages exert pro-inflammatory effects, while M2 macrophages promote anti-inflammatory responses, tissue repair and vascular remodeling (22). In normal pregnancy, M2-polarized dMφ are critical for maintaining immune tolerance, facilitating trophoblast invasion and enhancing endometrial receptivity (23). For example, a first-trimester study demonstrated that $CD14^+$ dMφ recruit extravillous trophoblasts to uterine spiral arteries, inducing apoptosis of vascular smooth muscle cells and enabling efficient vascular remodeling (24). Conversely, dysregulation of macrophage polarization is implicated in pregnancy complications. A murine model of inflammation-driven miscarriage, induced by low-dose lipopolysaccharide, revealed a pathological shift toward M1 dominance (elevated M1/M2 ratio) and reduced M2 macrophages, underscoring the detrimental impact of pro-inflammatory activation on pregnancy maintenance (25).

Successful embryo implantation is contingent upon a tightly regulated transient inflammatory phase within the endometrium, predominantly mediated by pro-inflammatory M1 macrophages (26). During early pregnancy, M1 macrophages not only facilitate embryo attachment but also confer antimicrobial protection at the maternal-fetal interface. Following trophoblast invasion into the endometrial stroma, a progressive shift toward M2 polarization occurs, characterized by enhanced expression of anti-inflammatory mediators (such as IL-10 and TGF-β) that promote apoptotic cell clearance, tissue remodeling

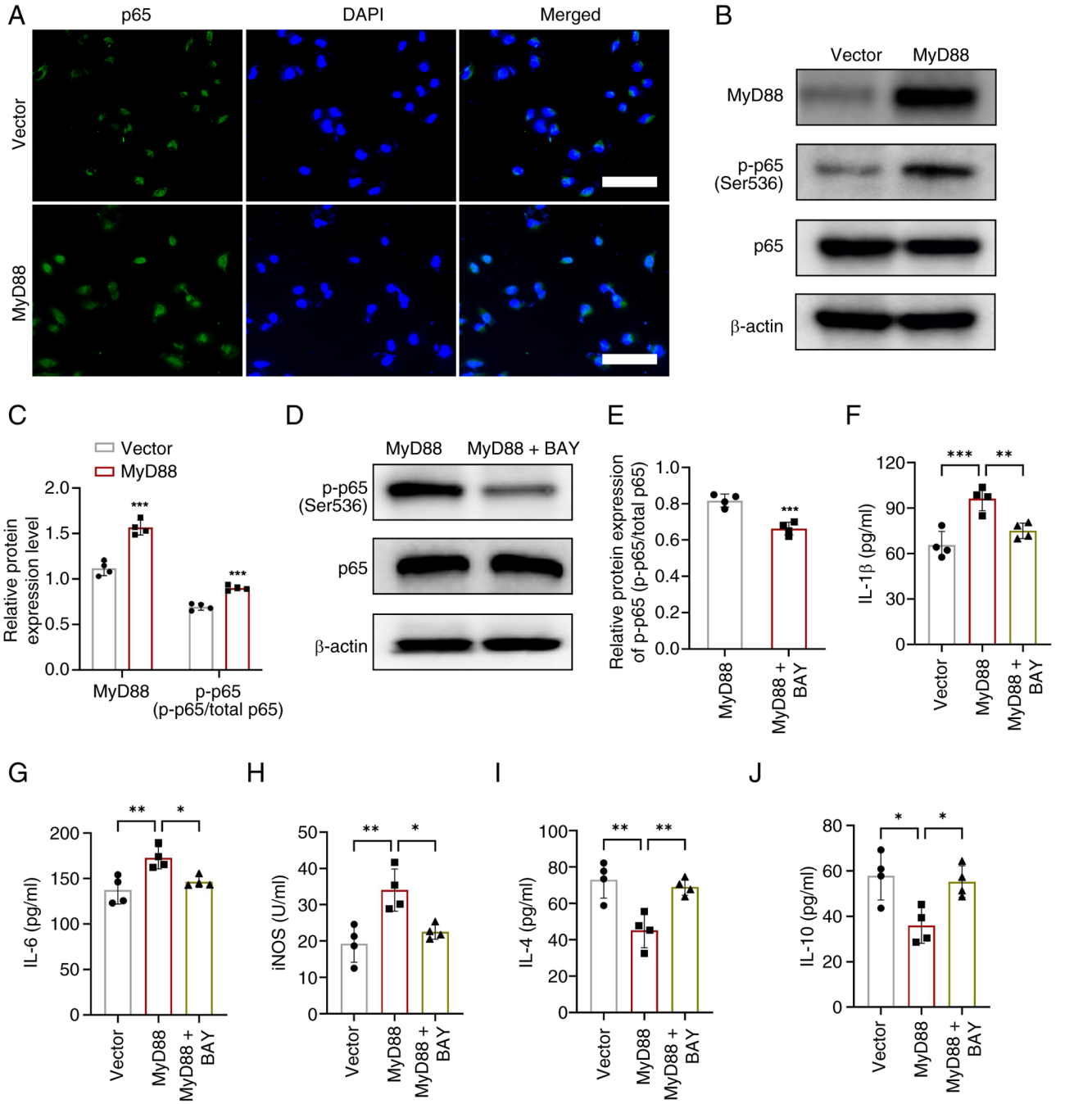



Figure 5. MyD88 overexpression promotes pro-inflammatory macrophage activation in THP-1 cells via p65 NF-κB. (A) Immunofluorescence analysis of the nuclear translocation of p65 NF-κB in MyD88-overexpressing THP-1-derived macrophages (scale bar, 50 $\mu$m). (B) Protein levels and (C) quantification of MyD88 ($^{***}$P<0.001, unpaired t-test; 95% CI, 0.3110 to 0.5890; $R^2$=0.9127) and p-p65 (p-p65/total p65; $^{***}$P<0.001, unpaired t-test; 95% CI, 0.1494 to 0.2656; $R^2$=0.9271) in MyD88-overexpressing THP-1-derived macrophages (n=4 independent experiments). (D) Protein expression and (E) quantification of p-p65 in MyD88-overexpressing THP-1-derived macrophages treated with the NF-κB inhibitor BAY 11-7082 (n=4 independent experiments) (p-p65/total p65; $^{***}$P<0.001, unpaired t-test; 95% CI, -0.2164 to -0.09362; $R^2$=0.8642). The content of the inflammatory mediators (F) IL-1β (one-way ANOVA with Tukey's test; MyD88 vs. vector: $^{***}$P<0.001; 95% CI, 15.63 to 45.47; MyD88 + BAY vs. MyD88: $^{**}$P<0.01; 95% CI, -36.09 to -6.258; $\varepsilon^2$=0.7587; $R^2$=0.7923), (G) IL-6 (one-way ANOVA with Tukey's test; MyD88 vs. vector: $^{**}$P<0.01; 95% CI, 12.21 to 58.84; MyD88 + BAY vs. MyD88: $^{*}$P<0.05; 95% CI, -49.69 to -3.060; $\varepsilon^2$=0.6853; $R^2$=0.6844) and (H) iNOS (one-way ANOVA with Tukey's test; MyD88 vs. vector: $^{**}$P<0.01; 95% CI, 5.636 to 23.91; MyD88 + BAY vs. MyD88: $^{*}$P<0.05; 95% CI, -20.66 to -2.386; $\varepsilon^2$=0.7273; $R^2$=0.7143) after BAY 11-7082 treatment in MyD88-overexpressing cells (n=4 independent experiments). The content of the anti-inflammatory cytokines (I) IL-4 (one-way ANOVA with Tukey's test; MyD88 vs. vector: $^{**}$P<0.01; 95% CI, -44.54 to -11.06; MyD88 + BAY vs. MyD88: $^{**}$P<0.01; 95% CI, 7.008 to 40.49; $\varepsilon^2$=0.7028; $R^2$=0.736) and (J) IL-10 (one-way ANOVA with Tukey's test; MyD88 vs. vector: $^{*}$P<0.05; 95% CI, -39.02 to -4.880; MyD88 + BAY vs. MyD88: $^{*}$P<0.05; 95% CI, 2.305 to 36.44; $\varepsilon^2$=0.5979; $R^2$=0.6312) after BAY 11-7082 treatment in MyD88-overexpressing cells (n=4 independent experiments). MyD88, myeloid differentiation primary response 88; p-, phosphorylated; iNOS, inducible nitric oxide synthase.

and immune tolerance (27). M2 macrophages further stabilize the gestational microenvironment by recruiting Th2 cells and polarizing them toward an immunoregulatory phenotype, thereby suppressing detrimental Th1/Th17 responses (28). This M2-dominant state is critical for maintaining pregnancy, as it establishes a protective, anti-inflammatory milieu that

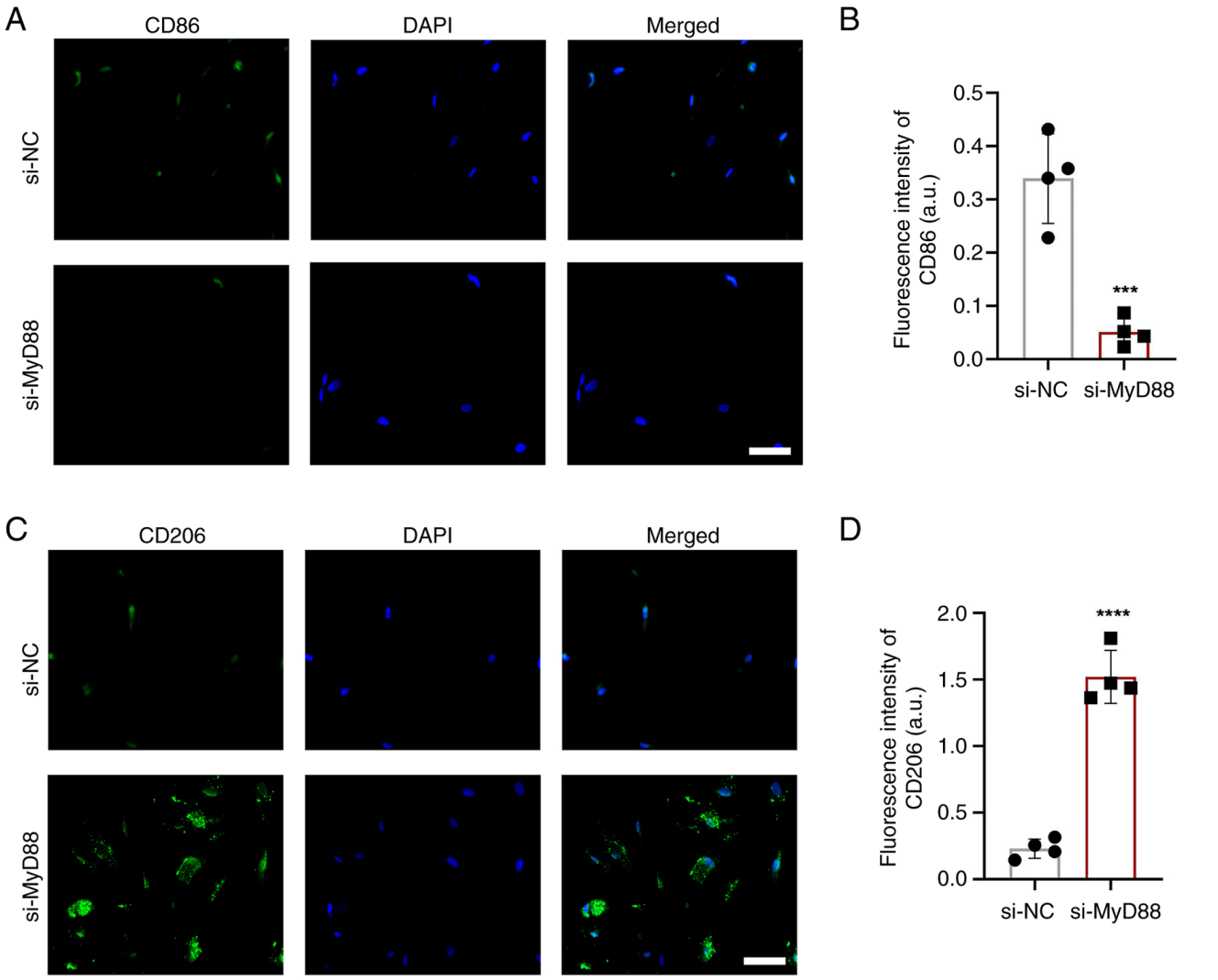



Figure 6. MyD88 knockdown suppresses M1 polarization while concurrently promoting M2 polarization in RAW264.7 cells. (A) Immunofluorescence staining of CD86 following si-MyD88 or si-NC treatment in RAW264.7 cells (scale bar, 50 $\mu$m). (B) The fluorescence intensity of of CD86 was determined following si-MyD88 treatment (n=4 independent experiments) ($^{***}$P<0.001, unpaired t-test; 95% CI, -0.3965 to -0.1800; $R^2$=0.8762). (C) Immunofluorescence staining of CD206 following si-MyD88 or si-NC treatment in RAW264.7 cells (scale bar, 50 $\mu$m). (D) The fluorescence intensity of CD206 was determined following si-MyD88 treatment (n=4 independent experiments) ($^{****}$P<0.0001, unpaired t-test; 95% CI, 1.032 to 1.551; $R^2$=0.9612). MyD88, myeloid differentiation primary response 88; si-, small interfering RNA; NC, negative control; CD, cluster of differentiation.

prevents fetal rejection. Near term, a physiological resurgence of M1 macrophages drives labor-associated inflammation and tissue breakdown (29). However, dysregulation of this dynamic balance is strongly associated with pathological pregnancies. In miscarriage, decidual tissues exhibit a pronounced M1/M2 imbalance, marked by elevated pro-inflammatory cytokines (such as TNF-α and IL-6) and reduced immunosuppressive factors (such as IL-10), which destabilize immune tolerance and impair placental development (30,31).

The findings of the present study reveal a robust and specific shift in dMφ polarization from an M2-like state toward an M1-like state in EPL. In normal gestation, M2-like macrophages, characterized by anti-inflammatory and immunoregulatory functions, facilitate immune tolerance, tissue remodeling and homeostasis at the maternal-fetal interface. By contrast, EPL decidua exhibits a pronounced shift toward M1-like polarization, marked by excessive secretion of pro-inflammatory cytokines (such as IL-1β and IL-6) and impaired immunosuppression, which destabilizes the gestational microenvironment and triggers inflammation-driven pregnancy failure. Notably, the complexity of macrophage polarization requires a rigorous phenotypic definition. By employing a four-marker refined gating strategy (including CD86, CD206, CD163 and CD209), the present study demonstrated that the polarized subsets, $CD86^+CD206^-CD163^-CD209^-$ M1-like and $CD86^-CD206^+CD163^+CD209^+$ M2-like macrophages, exhibited significant alterations in EPL. Notably, the proportion of the intermediate $CD86^+CD206^+$ mixed-phenotype population remained unchanged between groups. This suggests that the pathological imbalance in EPL is not merely an accumulation of transitional or mixed states, but rather a definitive and directional shift away from the M2-like program towards an M1-like pro-inflammatory state. Mechanistically, MyD88, a central adaptor in TLR signaling, was identified as a key regulator of this imbalance. Elevated MyD88 expression in EPL tissues was associated with M1 dominance, while knockdown of MyD88

in macrophages suppressed M1 markers (such as CD86, IL-1β and IL-6) and enhanced M2-associated factors (such as CD206, IL-4 and IL-10). This suggests that MyD88 amplifies TLR-mediated inflammatory cascades, skewing macrophages toward a pro-inflammatory phenotype in EPL. These insights bridge clinical observations (M1/M2 imbalance in EPL decidua) with molecular mechanisms (MyD88-driven polarization), offering a novel framework to understand immune dysregulation in pregnancy loss. By identifying MyD88 as a potential mediator of macrophage polarization, the present study highlights a promising avenue for future investigation into strategies that modulate macrophage equilibrium, which may eventually contribute to improving outcomes in high-risk pregnancies.

TLRs are expressed on various immune cell surfaces, including mast cells, dendritic cells and macrophages, which constitute the primary defense mechanism against pathogenic invasion (32). Notably, activation of the MyD88-dependent TLR4/MyD88/NF-κB signaling pathway has been implicated in disrupting immune homeostasis by inducing Th1/Th2 imbalance (33). MyD88 acts as a shared adaptor protein for both TLR4 and the IL-1R family. To determine whether the upregulation of MyD88 is specifically driven by TLR4 rather than a general inflammatory response mediated by other MyD88-dependent receptors, knockdown experiments targeting IL-1R were performed in the present study. Notably, while si-IL-1R successfully reduced IL-1R protein levels, it had no effect on MyD88 expression. This finding demonstrates that the elevated MyD88 expression in EPL is specifically driven by TLR4, rather than being a secondary consequence of IL-1R activation. This reinforces the notion that the TLR4-MyD88-NF-κB axis is a distinct and targeted mechanism underlying the inflammatory pathogenesis of EPL.

MyD88 plays a dual role in macrophage polarization, whereby its inhibition reduces CD86 expression while upregulating the M2-associated marker CD206 (34). Furthermore, MyD88 contributes to colitis-associated tumorigenesis by modulating macrophage polarization dynamics (35). The protein stability of MyD88 is regulated through ubiquitination mediated by E3 ubiquitin ligases (36), and MyD88-dependent osteopontin has been shown to drive M2 polarization via the STAT3/PPARγ pathway (35). Nevertheless, the involvement of MyD88-mediated macrophage polarization in EPL remains unexplored. To investigate the role of MyD88 in EPL pathogenesis, in the present study, MyD88 expression in decidual tissues was compared from normal first-trimester pregnancies and EPL cases. Immunohistochemical analysis revealed significantly elevated MyD88 protein levels in EPL decidua. Subsequent siRNA-mediated *MyD88* knockdown in Raw264.7 macrophages demonstrated distinct polarization shifts, whereby IL-4 and IL-10 (M2-associated cytokines) were markedly upregulated, whereas pro-inflammatory M1 markers (IL-1β, IL-6 and iNOS) and surface CD86 expression exhibited significant downregulation. These findings collectively suggest that MyD88 promotes M1 macrophage dominance while suppressing M2 polarization in the decidual microenvironment, potentially contributing to EPL pathophysiology. The limitations of the present study should be considered when interpreting the findings. Firstly, the cohort included both sporadic and recurrent EPL cases without stratification. The lack of stratification by recurrence history may have introduced additional variability into the analysis. Secondly, the *in vitro* experiments were performed using the murine macrophage RAW264.7 cell line and THP-1-derived human macrophages. While these cell lines are well-established and widely used models for studying macrophage polarization, they differ from primary human dMφ in origin and functional plasticity. Primary human dMφ are difficult to obtain in sufficient numbers and have a short *in vitro* lifespan, which restricts their use in experiments requiring genetic manipulation and multi-time-point pathway analysis; however, this practical constraint does not eliminate the need for validation in primary cells. Future studies should confirm the present findings in freshly isolated human dMφ.

In summary, the present study demonstrated that macrophage polarization played a pivotal role in maintaining immune tolerance at the maternal-fetal interface during normal pregnancy. By contrast, a pronounced increase in M1-like macrophage infiltration was observed in the decidua of EPL cases. Mechanistic investigations revealed that MyD88 activation promoted M1-polarized macrophage differentiation, thereby disrupting immune homeostasis and contributing to pregnancy failure. Notably, pharmacological or genetic inhibition of MyD88 attenuated pro-inflammatory M1 polarization while enhancing immunoregulatory M2 phenotypes, suggesting its critical role in sustaining decidual immune balance. These findings identify MyD88 as a key regulator of macrophage polarization in the decidua, with potential implications for understanding the immunopathology of EPL.

**Acknowledgements**

Not applicable.

**Funding**

The present study was supported by the Natural Science Foundation of Xinjiang Uygur Autonomous Region (grant no. 2022D01C592).

**Availability of data and materials**

The data generated in the present study may be requested from the corresponding author.

**Authors' contributions**

JJ, DW and YJ conceived the study, and wrote/revised the manuscript. JJ, XW, FW and DL conducted the experiments, and collected and analyzed data. NT collected and analyzed the data. JJ and YJ confirm the authenticity of all the raw data. All authors have read and approved the final manuscript.

**Ethics approval and consent to participate**

The study was approved by the Ethics Committee of the People's Hospital of Xinjiang Uygur Autonomous Region (approval no. KY2023060138). All patients involved in the study provided written informed consent.

## Patient consent for publication

Not applicable.

## Competing interests

The authors declare that they have no competing interests.

## References


1. Motan T, Cockwell H, Elliott J, Antaki R and White J: Guideline No. 464: Recurrent pregnancy loss. J Obstet Gynaecol Can 47: 103167, 2025.
2. Krashin JW, Black P, Brannen E, Gard CC, Lin Y, Greenwood-Ericksen M, Trujillo VY, Burkhardt G and Schreiber CA: Geographic access to early pregnancy loss management. Obstet Gynecol 143: 435-439, 2024.
3. Liu D, Huang X, Xu Z, Chen M and Wu M: Predictive value of NLR and PLR in missed miscarriage. J Clin Lab Anal 36: e24250, 2022.
4. Shao M, Zhang Y, Tang H, Zhou Z, Zhai M, Zhou X, Bi X, Liao J, Zhang C and Jiang L: Multi-omics insights into immune tolerance at the maternal-fetal interface in recurrent pregnancy loss: Mechanisms, integration challenges, and translational perspectives. Front Immunol 17: 1811970, 2026.
5. Duan H, Deng W, Kzhyshkowska J, Chen D and Zhang S: Macrophage at maternal-fetal Interface: Perspective on pregnancy and related disorders. Placenta 180: 87-99, 2026.
6. Zhao QY, Li QH, Fu YY, Ren CE, Jiang AF and Meng YH: Decidual macrophages in recurrent spontaneous abortion. Front Immunol 13: 994888, 2022.
7. Sun F, Wang S and Du M: Functional regulation of decidual macrophages during pregnancy. J Reprod Immunol 143: 103264, 2021.
8. Zhang L, Tian X, Liu M, Zong H, Yu W, Zheng C, Zhang D and Zhang H: Exosomal circDNAJB6 derived from decidual macrophages promotes preeclampsia progression via the miR-670-5p/TOB2 axis and by subsequently regulating the PPARγ/NF-κB pathway. J Transl Med 23: 1154, 2025.
9. Wang C, Ma C, Gong L, Guo Y, Fu K, Zhang Y, Zhou H and Li Y: Macrophage polarization and its role in liver disease. Front Immunol 12: 803037, 2021.
10. Liu J, Deng Y, Wang A, Liu B, Zhou X, Yin T, Wang Y, Tang T, Qiu Y, Chen J and Yang J: Investigation into the role of the MITA-TRIM38 interaction in regulating pyroptosis and maintaining immune tolerance at the maternal-fetal interface. Cell Death Dis 14: 780, 2023.
11. Liu S, Diao L, Huang C, Li Y, Zeng Y and Kwak-Kim JYH: The role of decidual immune cells on human pregnancy. J Reprod Immunol 124: 44-53, 2017.
12. Zhang Z, Lin W, Yan J, Wang X, Wang J, Wang F, He T, Xu J, Xia Y and Chen Y: Prenatal electroacupuncture modulates maternal-fetal immune activation via a brain-to-splenic signal. Cell Rep 44: 116576, 2025.
13. Chandrasekar SA, Palaniyandi T, Parthasarathy U, Surendran H, Viswanathan S, Wahab MRA, Baskar G, Natarajan S and Ranjan K: Implications of Toll-like receptors (TLRs) and their signaling mechanisms in human cancers. Pathol Res Pract 248: 154673, 2023.
14. Kao C, Wang SW, Chen PC, Huang CY, Wei YF, Ho CH and Hong YH: rice husk silica liquid enhances autophagy and reduces overactive immune responses via TLR-7 signaling in lupus-prone models. Int J Mol Sci 25: 10133, 2024.
15. Kim YC, Lee SE, Kim SK, Jang HD, Hwang I, Jin S, Hong EB, Jang KS and Kim HS: Toll-like receptor mediated inflammation requires FASN-dependent MYD88 palmitoylation. Nat Chem Biol 15: 907-916, 2019.
16. Schettino A, Saviano A, Marigliano N, Smimmo M, Esposito E, Begum J, Fatima A, Urbanowski AM, Mahony C, Khormi AM, *et al*: A Mangifera indica L. extract functions as a broad TLR2/4/6 signalling rheostat to attenuate MyD88/NF-κB-driven inflammation and macrophage polarization. Pharmacol Res 224: 108099, 2026.
17. Livak KJ and Schmittgen TD: Analysis of relative gene expression data using real-time quantitative PCR and the 2(-Delta Delta C(T)) Method. Methods 25: 402-408, 2001.
18. Shynlova O, Nedd-Roderique T, Li Y, Dorogin A, Nguyen T and Lye SJ: Infiltration of myeloid cells into decidua is a critical early event in the labour cascade and post-partum uterine remodelling. J Cell Mol Med 17: 311-324, 2013.
19. Lakatos KF, Hasselblatt K, Fülöp V, Végh GL, McElrath T, Berkowitz RS and Elias KM: Isolation and culture of decidual natural killer cells from term placenta and complete hydatidiform mole. J Reprod Immunol 150: 103475, 2022.
20. Li X, Li X, Huang P, Zhang F, Du JK, Kong Y, Shao Z, Wu X, Fan W, Tao H, *et al*: Acetylation of TIR domains in the TLR4-Mal-MyD88 complex regulates immune responses in sepsis. EMBO J 43: 4954-4983, 2024.
21. Zhao F, Guo Z, Hou F, Fan W, Wu B and Qian Z: Magnoflorine alleviates 'M1' polarized macrophage-induced intervertebral disc degeneration through repressing the HMGB1/Myd88/NF-κB pathway and NLRP3 inflammasome. Front Pharmacol 12: 701087, 2021.
22. Lash GE, Pitman H, Morgan HL, Innes BA, Agwu CN and Bulmer JN: Decidual macrophages: Key regulators of vascular remodeling in human pregnancy. J Leukoc Biol 100: 315-325, 2016.
23. Pique-Regi R, Romero R, Tarca AL, Sendler ED, Xu Y, Garcia-Flores V, Leng Y, Luca F, Hassan SS and Gomez-Lopez N: Single cell transcriptional signatures of the human placenta in term and preterm parturition. Elife 8: 52004, 2019.
24. Zhu J, Song W, Xu S, Ma Y, Wei B, Wang H and Hua S: Shenfu injection promotes vasodilation by enhancing eNOS activity through the PI3K/Akt signaling pathway in vitro. Front Pharmacol 11: 121, 2020.
25. Ji WH, Li DD, Wei DP, Gu AQ, Yang Y and Peng JP: Cytochrome P450 26A1 modulates the polarization of uterine macrophages during the peri-Implantation period. Front Immunol 12: 763067, 2021.
26. Xu L, Li Y, Sang Y, Li DJ and Du M: Crosstalk between trophoblasts and decidual immune cells: The cornerstone of maternal-fetal immunotolerance. Front Immunol 12: 642392, 2021.
27. Li ZH, Wang LL, Liu H, Muyayalo KP, Huang XB, Mor G and Liao AH: Galectin-9 alleviates LPS-induced preeclampsia-like impairment in rats via switching decidual macrophage polarization to M2 subtype. Front Immunol 9: 3142, 2018.
28. Yang C, Li W, Liu X, Ma Z, Chen J, Gong Q, Braunstein Z, Rao X, Wei Y and Zhong J: Immune dysregulation at the maternal-fetal interface exacerbates adverse pregnancy outcomes in an inflammatory arthritis murine model. Biomedicines 13: 1440, 2025.
29. Shan Y, Shen S, Long J, Tang Z, Wu C and Ni X: Term and preterm birth initiation is associated with the macrophages shifting to M1 polarization in gestational tissues in mice. Biology (Basel) 11: 1759, 2022.
30. Liu H, Chen H, Han T, Wang X, Dai J, Yang X, Chan S, Cannon RD, Yang Y, Mousa H, *et al*: Lipid imbalance and inflammatory oxylipin cascade at the maternal-fetal interface in recurrent spontaneous abortion. Heliyon 10: e40515, 2024.
31. Xiao Y, Zeng FY, Liu JS, Zhao F and Sun JL: Recent developments in macrophages imbalance and recurrent spontaneous abortion. J Immunol Res 2026: e8862057, 2026.
32. Fitzgerald KA and Kagan JC: Toll-like receptors and the control of immunity. Cell 180: 1044-1066, 2020.
33. Lu H, Xu X, Fu D, Gu Y, Fan R, Yi H, He X, Wang C, Ouyang B, Zhao P, *et al*: Butyrate-producing eubacterium rectale suppresses lymphomagenesis by alleviating the TNF-induced TLR4/MyD88/NF-κB axis. Cell Host Microbe 30: 1139-1150.e7, 2022.
34. Zhang J, Liu Y, Chen H, Yuan Q, Wang J, Niu M, Hou L, Gu J and Zhang J: MyD88 in hepatic stellate cells enhances liver fibrosis via promoting macrophage M1 polarization. Cell Death Dis 13: 411, 2022.
35. Yuan Q, Gu J, Zhang J, Liu S, Wang Q, Tian T, Chen Z and Zhang J: MyD88 in myofibroblasts enhances colitis-associated tumorigenesis via promoting macrophage M2 polarization. Cell Rep 34: 108724, 2021.
36. Strickson S, Emmerich CH, Goh ETH, Zhang J, Kelsall IR, Macartney T, Hastie CJ, Knebel A, Peggie M, Marchesi F, *et al*: Roles of the TRAF6 and Pellino E3 ligases in MyD88 and RANKL signaling. Proc Natl Acad Sci USA 114: E3481-E3489, 2017.


Copyright © 2026 Jiao et al. This work is licensed under a Creative Commons Attribution-NonCommercial-NoDerivatives 4.0 International (CC BY-NC-ND 4.0) License.